TRIPLE FLAMES IN MICROGRAVITY FLAME SPREAD

Indrek S. Wichman
Michigan State University
East Lansing, Michigan

Introduction

It has become apparent from recent work, for both opposed and coflow flame spread (refs. 1-4), that the flame tip controls much of the subsequent flame spread dynamics. The "flame anchoring region" or "lean-limit zone" or "weakly premixed flame foot zone" of the late 1970s and early 1980s has acquired a definite theoretical structure, commonly referred to as the "triple flame". Though its existence is unquestionably acknowledged, its importance in practical situations of flame attachment, flame spread, etc. has not been clearly established.

The purpose of this project is to examine in detail the influence of the triple flame structure on the flame spread problem. It is with an eye to the practical implications that this fundamental research project must be carried out. The microgravity configuration is preferable because buoyancy-induced stratification and vorticity generation are suppressed. A more convincing case can be made for comparing our predictions - which are zero -g - and any projected experiments.

Our research into the basic aspects will employ two models, both of the general kind illustrated in Fig. 1. In one, flows of fuel and oxidizer from the lower wall are not considered. In the other, a convective flow is allowed, see Fig. 1. The non-flow model allows us to develop combined analytical and numerical solution methods that may be used in the more complicated convective-flow model.

Zero-Flow Model:

A preliminary analysis of this model is found in ref. 5. We are presently developing a more comprehensive version. The difficult part occurs in the construction of the outer solution, which must be matched to the inner flame-zone solution. The forward flame zone, in which the reaction rate is a maximum, is the elliptic (2-D) triple point region. Downstream of this is the trailing diffusion flame (DF). The elliptic, non-linear triple-point-zone equation must possess spatial boundary conditions on all of its four sides. The top side is straightforward, the two lateral sides are more difficult. The bottom side is by far the most difficult. Here, the nonlinear elliptic triple-point-zone equation must match to the homogeneous quenching-zone solution (there

is no reaction here). But this region itself cannot be solved unless a suitable set of boundary conditions at its top edge is found (see Fig. 2). An iterative solution method must be employed. A "reasonable" boundary condition is postulated for the top of the quench zone. Then the quench equation is solved. The inner-zone equation is matched to this and the other outer-zone solutions. A new and more accurate temperature distribution across the lower zone is obtained, the quench zone equations are solved and the process is repeated. The solution can be compared with the full numerical solution for the quenching distance and the quenching temperature, as well as heat fluxes to the solid boundaries.

Convective-Flow Model:

Most of our effort on this project has centered on the convective flow case. We have developed a numerical solution code with variable meshes and other numerical refinements. The model problem is identical to the zero-flow case except for the presence of the constant convective flow from the lower reservoirs. A somewhat artificial zero-infiltration boundary conditions is applied, as in the zero-flow case [i.e., neither species can diffuse into the other stream prior to its arrival through the exit plane]. By numerical experimentation, we have determined that the triple flame structure is most clearly evident when both the nondimensional activation energy β and the Damköhler number D are large. As D increases, the flame tip moves closer to the cold wall. This can be offset by increasing the flow rate ε. When the increases of ε and D are coordinated in order to keep the stand-off (or quenching) distance constant, the triple flame structure becomes prominent. In our notation, D and ε are independent of one another, since length scales are measured with the burner width. Hence, an increase of ε for fixed D merely shifts the entire structure further downstream, whereas an increase of D (for fixed ε) moves it closer to the cold surface while simultaneously shrinking it laterally. In neither of these cases is the triple flame structure prominent. We can compare the sequences of figures given by Figs. 3.a-c, 4.a-c, 5.a-c. See also the full plots of temperature and fuel and oxidizer mass fractions in Figs. 6.
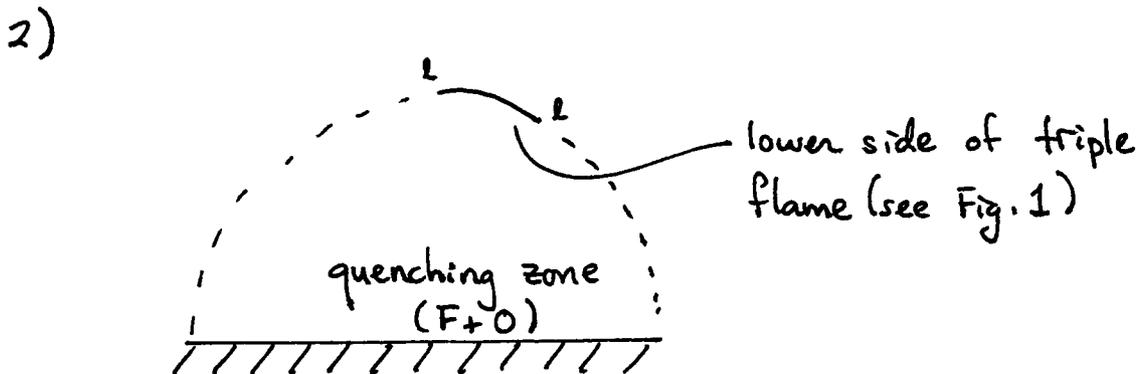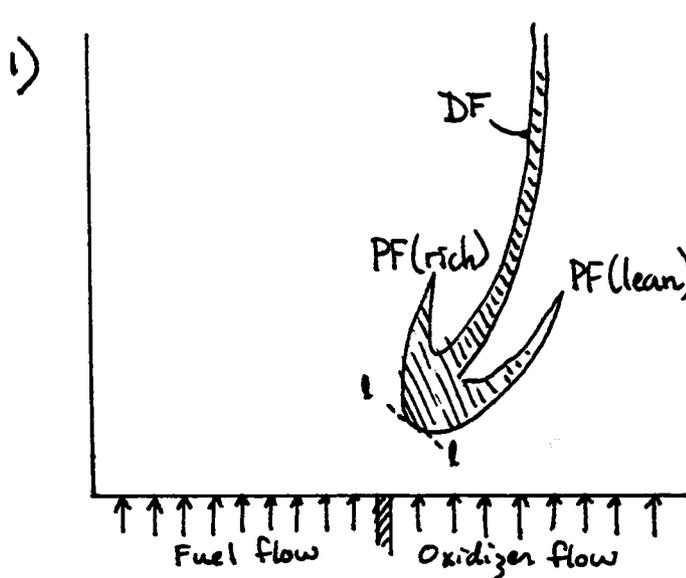
Once the fundamental details of the zero-flow model are clarified, similar methods may be applied to the convective flow model.

Simplified Flame Spread Model

Here we examine a simple solution for the mixture fraction, Z, for the case of a model configuration that resembles the flame spread problem. A discussion, and some results, for this simple model are given in ref. 6. Once the Z contours are calculated (we vary the input of fuel from the fuel wall, see Fig. 7), we choose a constant-Z flame contour (see Fig. 7) onto which we superpose the flame quenching information from the two previous model problems and the flame-shape information. In this way, a set of hypothetical flame shape plots can be made, as shown in Fig. 7. These can be used to aid in the prospective experimental visualization of triple flame structures in actual flames. It may also provide clues for why these structures are very difficult to see in practice for flame spread over solid fuels. For liquid fuels, triple flame structures can actually be observed, see ref. 7.

References

1. Agrawal, S., and Atreya, A., "Wind-Aided Flame Spread over an Unsteadily Vaporizing Solid," Twenty Fourth Symposium (International) on Combustion, The Combustion Institute, Pittsburgh, PA, 1992, pp. 1685-1693.
2. Wichman, I.S., and Agrawal, S., "Wind-Aided Flame Spread over Thick Solids," Combustion and Flame, 83, 1991, pp. 127-145.
3. Bhattacharjee, S., "A Comparison of Numerical and Analytical Solution of Creeping Flame Spread over Thermally Thin Material," Comb. and Flame, 93, 1993, pp. 434-444.
4. Delichatsios, M. A., "Comments on 'A Comparison of Numerical and Analytical Solution of Creeping Flame Spread over Thermally Thin Materials' by S. Bhattacharjee," Comb. and Flame, 95, 1993, pp. 336-339.
5. Wichman, I.S., "On the Quenching of a Diffusion Flame Near a Cold Wall," Combust. Sci. Tech., 64, 1989, pp. 295-313.
6. Wichman, I.S., "Theory of Opposed Flow Flame Spread," Prog. Energy Combust. Sci., 18, 1992, pp. 553-592.
7. Ross, H. D., "Ignition of and Flame Spread over Laboratory-Scale Pools of Pure Liquid Fuels," Prog. Energy Combust. Sci., 20, 1994, pp. 17-63.
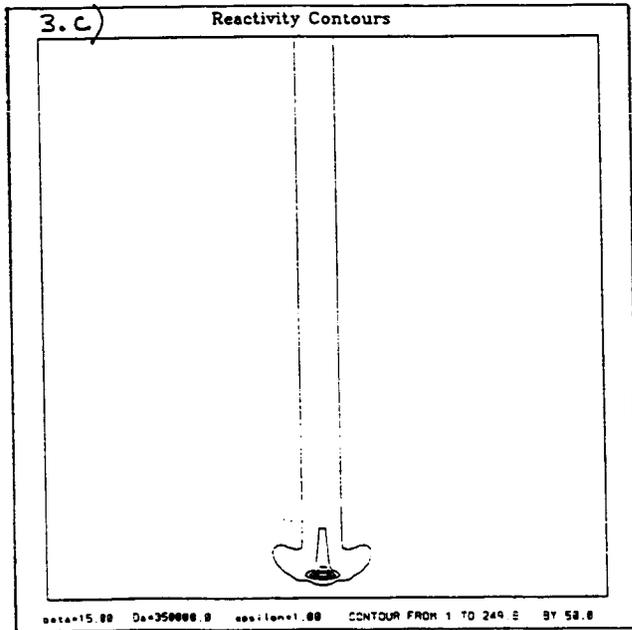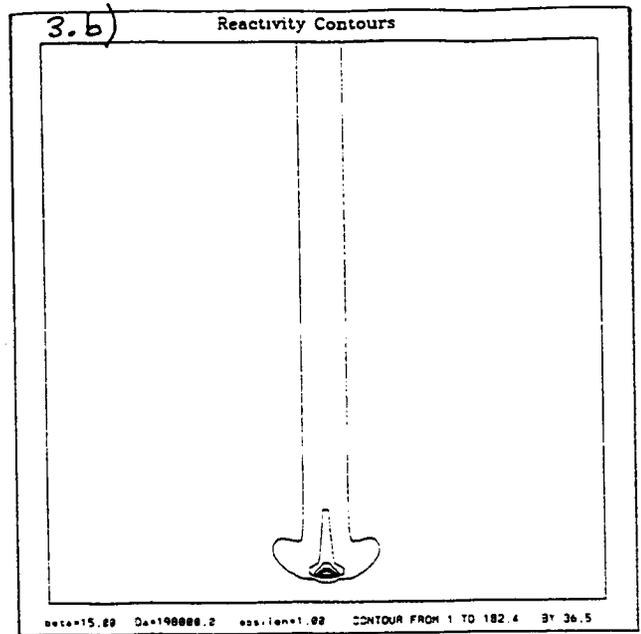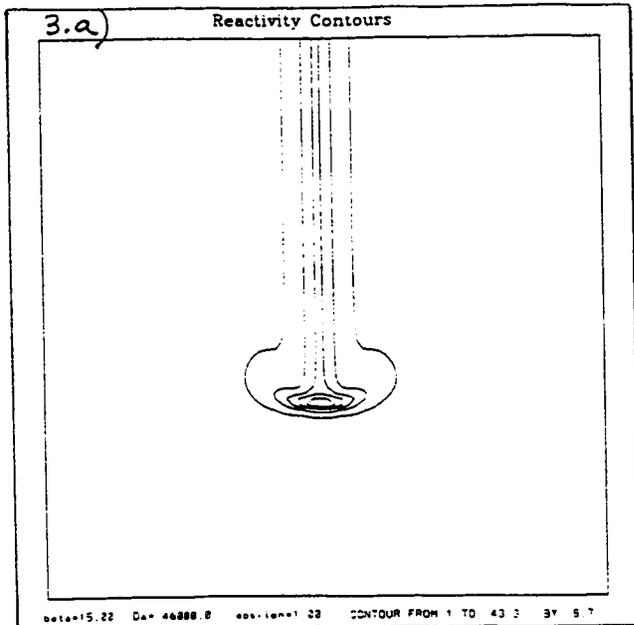
1)

DF

PF(rich)   PF(lean)

Fuel flow   Oxidizer flow

2)

lower side of triple flame (see Fig. 1)

quenching zone
(F+O)

3.a) Reactivity Contours

beta=15.22 Da=46000.0 epsilon=1.00 CONTOUR FROM 1 TO 43.3 BY 5.7

3.b) Reactivity Contours

beta=15.00 Da=190000.2 epsilon=1.00 CONTOUR FROM 1 TO 182.4 BY 36.5

3.c) Reactivity Contours

beta=15.00 Da=350000.0 epsilon=1.00 CONTOUR FROM 1 TO 249.5 BY 50.0

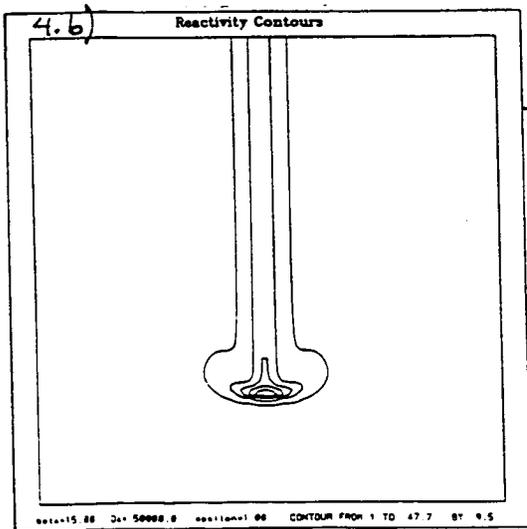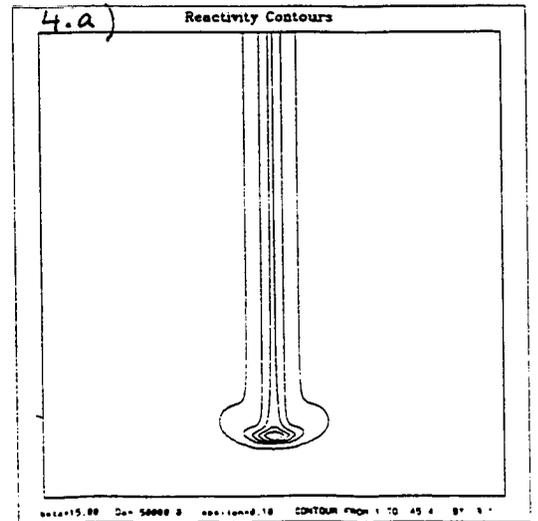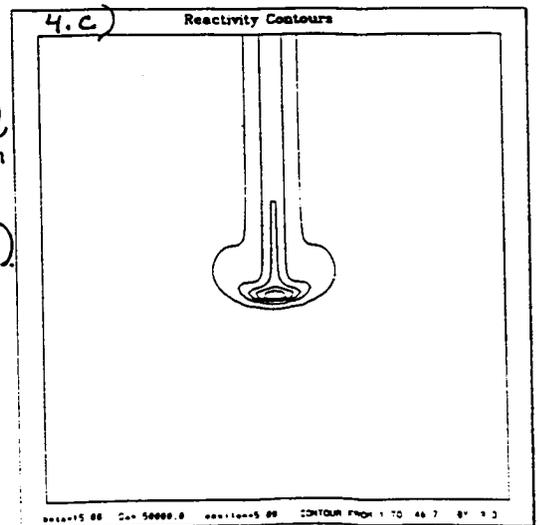**Fig. 3.a,b,c.** Fix β, fix ϵ, vary D from 46,000 to 350,000.

4.a) Reactivity Contours

beta=15.00 Da=50000.0 epsilon=0.10 CONTOUR FROM 1 TO 45.4 BY 1

4.b) Reactivity Contours

beta=15.00 Da=50000.0 epsilon=1.00 CONTOUR FROM 1 TO 47.7 BY 9.5

Fig. 4.a,b,c.
Fix β, fix D, vary ϵ from 0.1 to 5.0 ($\epsilon = 0.1, 1.0, 5$)

4.c) Reactivity Contours

beta=15.00 Da=50000.0 epsilon=5.00 CONTOUR FROM 1 TO 46.7 BY 9.3

242

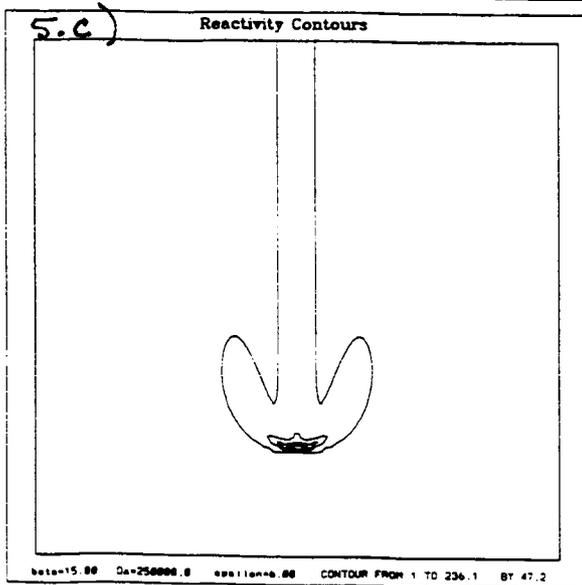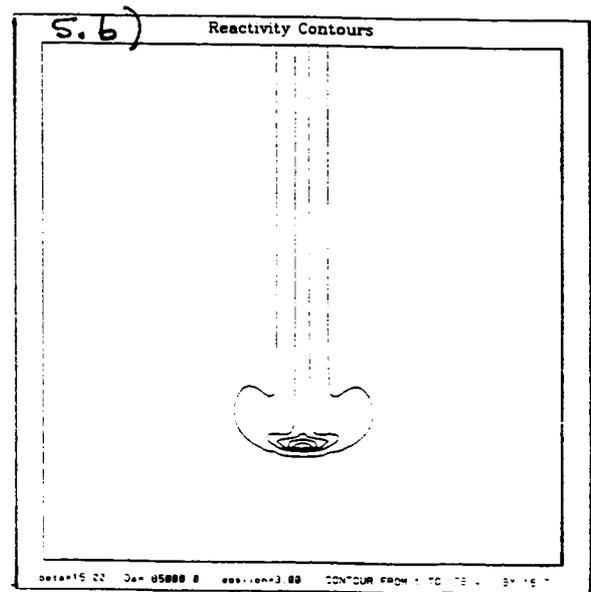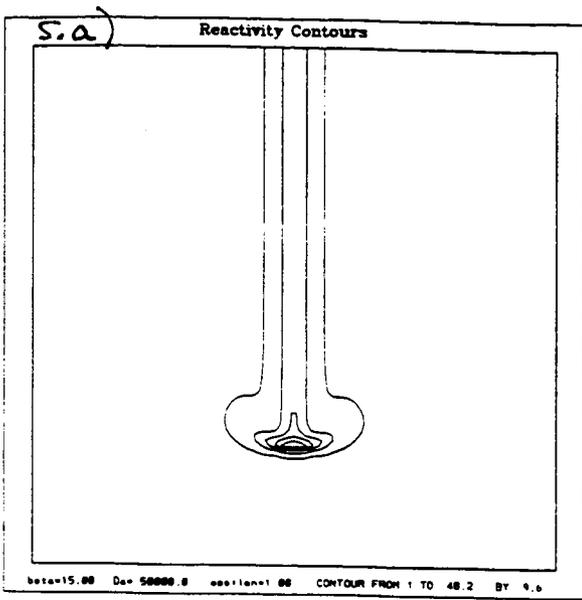Fig. 5.a,b,c: Fix $\beta = 15$, vary ϵ and D so that stand-off distance is fixed.

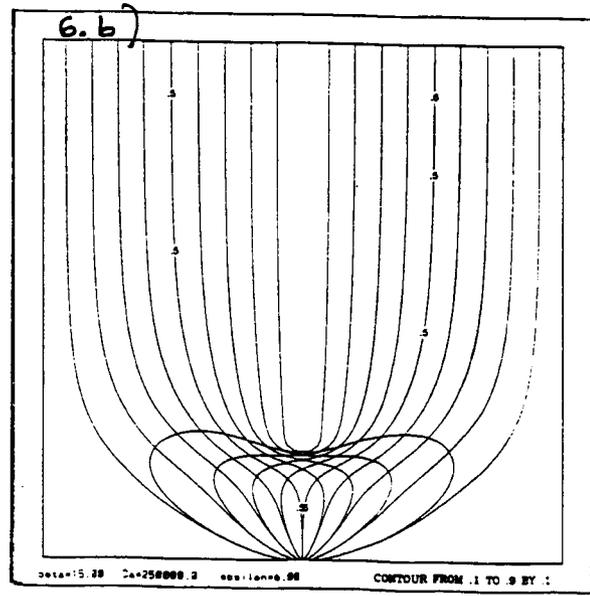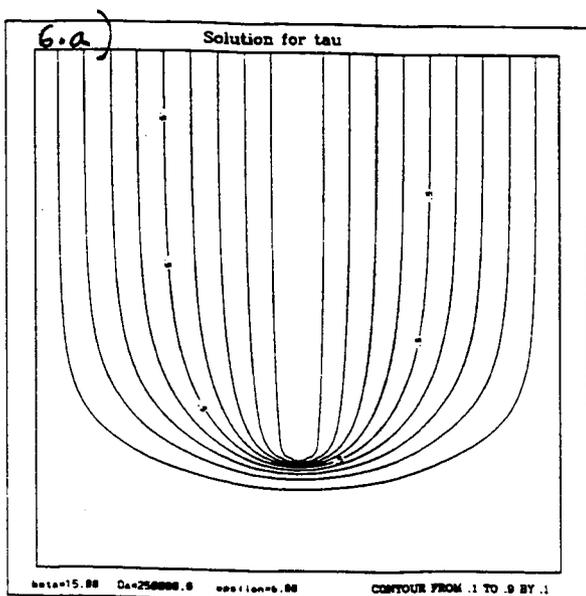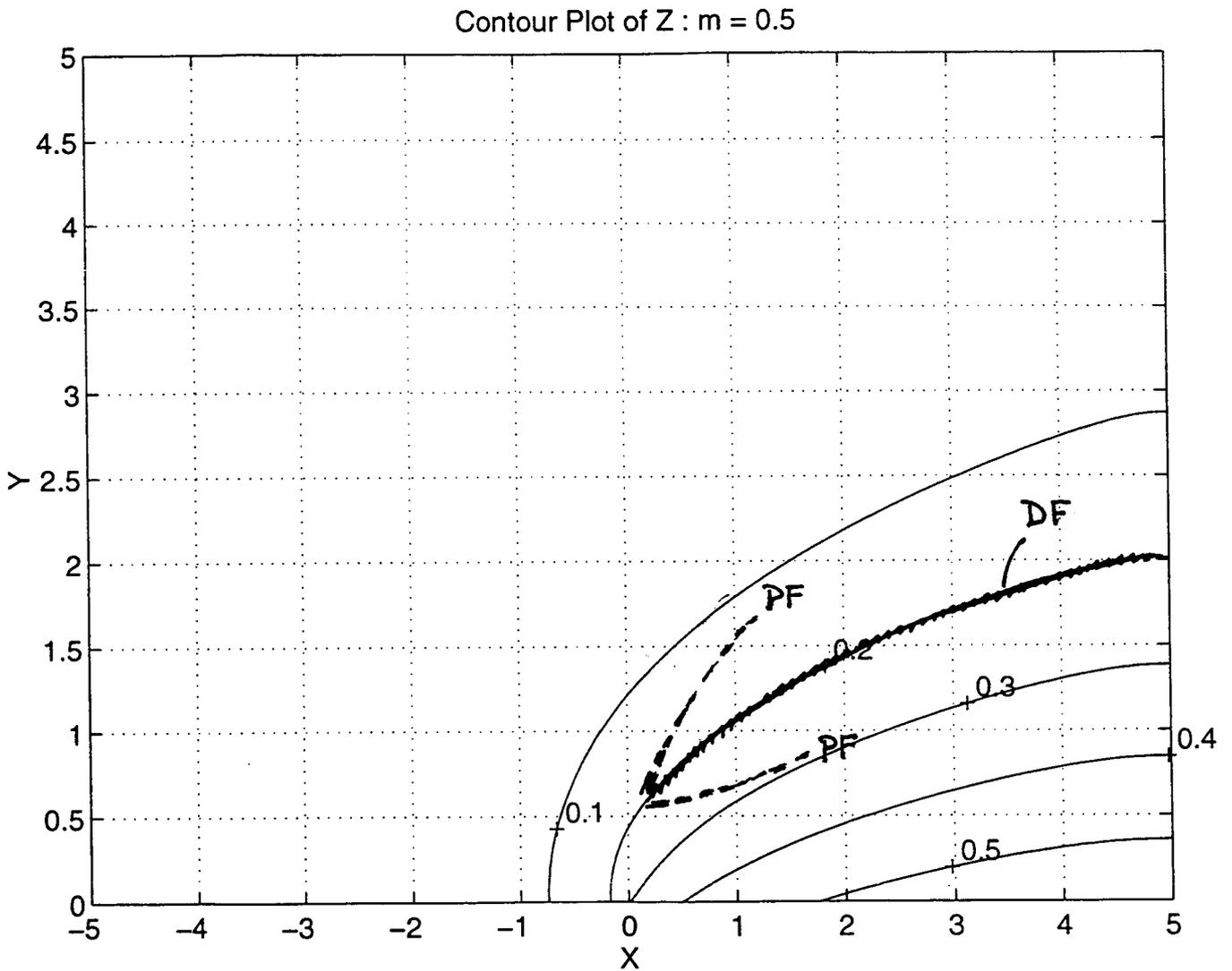Fig. 6.a,b: Contours of constant τ, y_0, y_F.

7)

Contour Plot of Z : m = 0.5

Fig. 7 : Contours of Z = constant for a mock flame-spread problem, onto which is superposed a flame structure $(Z = 0.2)$.